Hindawi
Shock and Vibration
Volume 2019, Article ID 7381852, 15 pages
https://doi.org/10.1155/2019/7381852

*Research Article*

# Improvement on Structural Forms of Pile Group Foundations of Deepwater Bridges

**Enbo Yu, Sen Ren, Haojun Tang, Yongle Li, and Chen Fang**

*Department of Bridge Engineering, Southwest Jiaotong University, Chengdu 610031, China*

Correspondence should be addressed to Haojun Tang; thj@swjtu.edu.cn

Received 8 March 2019; Revised 30 June 2019; Accepted 22 July 2019; Published 14 August 2019

Academic Editor: Zhixiong Li



As long-span cross-sea bridges extend to deeper sea areas, the bridge pile tends to increase in its slenderness ratio and becomes more susceptible to waves. To improve the structural stability at the construction stage, this study analyses wave-induced response of foundations. The wave theory and the method used for computing wave forces on foundations are first introduced. Then, a pile group foundation is taken as the research object, and different pile lengths ranging from 16 m to 46 m are considered. The wave-induced response of the piles and the cap is calculated. After understanding the effect of the pile length, three optimized foundations are proposed with the aim of reducing the free length of the pile, and the corresponding finite element models are established to compare their wave-induced response. The results show that the displacement at the top of the foundation increases with the increase in the pile length until the cap partly emerges from water and so does the internal force at the bottom. Setting a constraint in the middle of the piles can reduce their free lengths and is favourable to the wave-induced response of the foundation except for the shearing force. A stronger constraint shows better effects on improvement of the stability of the foundation. The conclusions provide reference for optimization on pile foundations of deepwater bridges.

## 1. Introduction

With the rapid development of construction technology, an increasing number of long cross-sea bridges have been constructed, greatly promoting the transportation and the economy in coastal areas. For instance, the Chesapeake Bay Bridge completed in 1964 connects the banks of the Chesapeake Bay. The Great Belt Bridge completed in 1998 crosses the Great Belt Strait. The Oresund Bridge completed in 2000 associates Denmark with Sweden. The Pingtan Strait Bridge and the Hong Kong–Zhuhai–Macao Bridge were completed in 2010 and 2018, respectively. As the weather condition and hydrological environment are more complicated, cross-sea bridges may be subject to strong winds with huge waves and prone to vibrate, affecting the structural stability and the running safety of vehicles [1, 2]. Apparently, the foundation is the key structure supporting the pier and the superstructure, so its dynamic response closely associates with the vibration of the whole structure and so does the vehicle. The deeper the water is, the longer the foundation could be, and thereby, its dynamic response becomes more obvious. In the construction stage when its top is not yet constrained by the pier, the freestanding foundation can be regarded as a cantilever. Although the vehicle is not involved at this situation, possible vibration of the foundation has potential effects on the construction of the pier. In general, the wave is accompanied with the wind, but the foundation is almost or even totally submerged in water, so it is more sensitive to effects of waves, while less affected by winds. In the service stage, a rigid foundation which can better resist strong waves is also favourable to its own safety as well as the stability of bridges and does the vehicle travelling through.

Apparently, the accurate simulation of the wave load is the basis of evaluation of structural response under waves. As for the expression of the wave motion, a linear wave theory which uses the potential function was proposed in 1845 [3]. The Stokes wave which assumes the wave motion as potential motion and belongs to finite amplitude theory was then proposed [4]. After that, the second-order, third-order, and fifth-order Stokes wave were successively derived [5, 6].

The motion of waves was also described using the elliptical cosine wave theory [7]. On the basis of this, the theory was further studied by other scholars and engineers so that it can be better applied in practice [8–10]. With the development of computer technology, the numerical simulation becomes an effective way to achieve the target [6, 11, 12]. As for the computation of fluid-structure interaction, the method proposed by Morison et al. [13] is used for calculating the wave force on the small-scale structure, while the theory of diffraction put forward by MacCamy and Fuchs [14] is used for the large-scale structure.

The dynamic response of offshore structures has attracted great attention of designers and scholars, especially for offshore wind turbines [15, 16]. Wave loads acting on the lower part below the water surface and wind loads acting on the upper part above the water surface play important roles. Adhikari and Bhattacharya [17] showed that the natural frequency of the turbine tower decreases with the decrease in stiffness of the foundation and the increase in axial load. Zhang et al. [18] investigated the dynamic response of a floating foundation of a turbine in 60 m deepwater and pointed out that the semisubmersible floating foundation can work with significant wave height less than 4 m. Wei et al. [19] computed the capacity of monopile- and jacket-supported wind turbines and found that structural response can be dominated by either the wind or the wave depending on structural characteristics and site conditions. Wang et al. [20] studied the dynamic response of a monopile-supported wind turbine subjected to wind, wave, and earthquake actions and indicated that it is necessary to consider the combination of the three actions in the design of such a turbine. Bachynski et al. [21] further studied the response of a monopile-supported wind turbine subjected to irregular wave loads, and the experimental results highlighted the resonant response of the monopile when subjected to severe wave loads. Sarmiento et al. [22] validated a multiuse floating platform which combines wave energy converters and wind harvesting. Wu et al. [23] discussed geotechnical and structural issues affecting the foundation of the offshore wind turbine. It is concluded that the foundation presents one of the main challenges in the design.

The bridge foundation has a variety of forms such as the caisson foundation, the tube caisson foundation, and the open caisson foundation. When the water is deep, the pile foundation, which consists of a group of bored piles extending to soil at the bottom and connected to a large cap at the top, has widely been used owing to its convenient construction and good adaptability [24–26]. However, it is difficult to model the precise dynamic response of the pile foundation under various dynamic loads due to large dimensions, structural complexity, and three-dimensional characteristics [27]. On the basis of the bridge foundation designed for the East Sea Bridge, Liu et al. [28] investigated the wave current forces on the pile foundation and examined the group effectiveness and the reduction coefficient for engineering design. Yao et al. [29] numerically simulated a super-long pile foundation in stratified soils under both vertical and lateral loads and concluded that the sleeved pile group can significantly reduce the horizontal displacement. Deng et al. [30] experimentally studied the effect of fluid-structure interaction on the modal dynamic response of a bridge pier supported by the pile foundation and found that the effect increases with the rise in water level, especially when the pier body is submerged in water. Deng et al. [31] further experimentally studied the modal dynamic response of a hollow bridge pier with the pile foundation submerged in water and provided better understanding of the effect of fluid-structure interaction. Deng et al. [32] investigated the cap effect on wave loads on piles, and the force-increasing effect on piles was observed when the relative cap dimension is small. In addition, Ya et al. [33] found that the dynamic response of a pile-cap structure under random sea wave action is the largest. Tomisawa and Kimura [34] proposed new techniques to improve seismic performance of the pile foundation for long life bridges. The seismic excitation on the pile foundation was also considered in some studies [35, 36].

The aforementioned studies have improved our understanding of the dynamic response of the pile foundation, but optimization on the form has not yet been fully explored. With long-span bridges extending to deeper sea areas, the length of the pile has to be increased, leading to more slender and flexible foundations. To reduce the structural dynamic response, optimization on the pile foundation with longer piles becomes important. Taking a long-span deepwater bridge into account, this paper studies the wave-induced response of a pile group foundation using ANSYS software and further optimizes the structural form. The main content is organized as follows. The wave loads on the piles and cap of the foundation are computed in Section 2. Five finite element models with different pile lengths are established, and their wave-induced vibration is compared and discussed in Section 3. After determining the relationship between the dynamic response and the pile length, the foundation is optimized with different structural forms in Section 4, and the effectiveness is evaluated by comparing the changes in the dynamic characteristics, including the cap's displacement and the piles' internal forces. Finally, some main conclusions are drawn in Section 5, providing reference for optimization on pile foundations of deepwater bridges.

## 2. Wave Force on the Foundation

*2.1. Case Description.* The engineering background of the paper is a deepwater long-span cable-stayed bridge with a total length of 1188 m, and its main span length is 532 m. The overall layout is shown in Figure 1. The measured data of the bridge location show that, in a-hundred-year return period, the wave on the transverse bridge direction has the maximum height $H$ of 9.69 m. The wave period $T$ is 10.8 s, and the wave circle frequency $\omega = 0.581$ rad/s. According to the dispersion relation, the wavelength is about 169 m. The density of seawater $\rho$ takes 1000 kg/m$^3$, and the water depth $d$ is considered as 45 m after flushing.

The bridge is supported by six pile group foundations marked with N01~N06 among which N03 and N04 are the main ones. Each of the six pile foundations consists of a group of piles and a cap on the top (Figure 1). In particular,

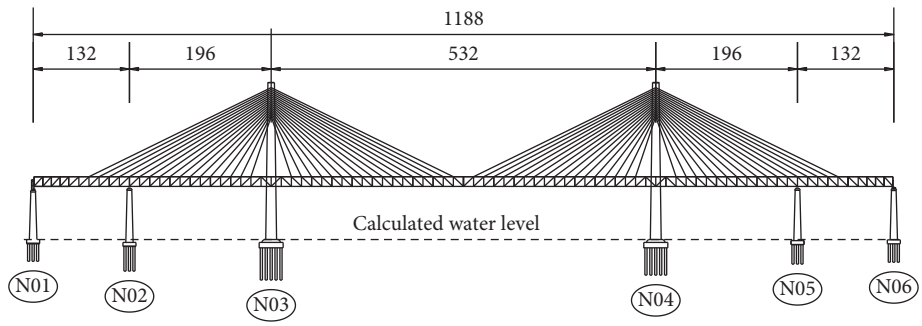


Figure 1: Layout of the target bridge (unit: m).

N03 has the longest free length in water, so it is easier to be affected by the wave force. Because of this reason, the subsequent analysis of this paper will be carried out around the N03 pile foundation. The cap dimension of N03 is 81.2 m × 33.2 m and the thickness is 7.5 m. The immense cap is submerged in water and supported by as much as 38 bored piles each of which has a diameter of 3 m. The basic cross-sectional design and the pile numbers are shown in Figure 2(a). For the deepwater pile foundation, the pile length is a key parameter in its design because long piles and short piles have their own advantages and disadvantages. To study the effect of the pile length on wave-induced response of the foundation, the length of N03 is decreased and increased, respectively. Five lengths ranging from 16 m to 46 m until the cap completely emerges from water are selected, as shown in Figure 2(b). It should be noted that the study mainly focuses the foundation itself, and the difference in construction is not considered for a fair comparison.

*2.2. Wave Forces on the Pile.* As discussed previously, the accurate simulation of the wave load is the basis of evaluation of structural response. Here, two indicators $H/gT^2$ and $d/gT^2$ where the parameters were defined and the corresponding values at the bridge site were given in Section 2.2 are computed. According to Le Méhauté's map and theory [37], the results show that the linear wave theory is applicable as the water is deep enough (Figure 3(a)). With the aim of comparing the wave-induced response for different forms of foundations, the linear wave theory is adopted in this paper. Therefore, velocity $u_x$ and acceleration $a_x$ of the wave can be expressed by the following equations in consideration of the dispersion relationship:

$$u_x = \frac{\partial \Phi}{\partial x} = \frac{\pi H}{T} \frac{\cosh k(z+d)}{\sinh kd} \cos(kx - \omega t), \quad (1)$$

$$a_x = \frac{\partial u_x}{\partial t} = \frac{2\pi^2 H}{T^2} \frac{\cosh k(z+d)}{\sinh kd} \sin(kx - \omega t), \quad (2)$$

where $\Phi$ is the velocity potential function; $z$ is the depth of the water particle when the origin of coordinates is set on the hydrostatic surface, $k$ is the number of fluctuations in the length of $2\pi$; $x$ is the horizontal coordinate; and the remaining parameters are unchanged.

For a cylinder, the structure with $D/L \leq 0.2$ is usually defined as a small-scale structure, and the structure with $D/L > 0.2$ is defined as a large-scale structure, where $D$ is the horizontal dimension of the structure and $L$ is the wavelength. Specially, the piles of N03 have a $D/L$ of 0.018, so the wave force can be calculated according to the theory proposed by Morison, as shown in Figure 3(b). When the origin of coordinates is set on the seabed, the wave force of the single pile at the height $z$ is expressed as follows:

$$f_H = f_D + f_I = \frac{1}{2} C_D \rho A u_x |u_x| + C_M \rho V_0 \frac{du_x}{dt}, \quad (3)$$

where $f_D$ and $f_I$ are the drag and the inertia forces and $C_D$ and $C_M$ are the corresponding coefficients, respectively, which are set as 1.2 and 2.0 according to Chinese code [38]. Taking a pile of N03 as an example and dividing it into different parts each of which has a unit length (Figure 4(b)), the time series of $f_D$ and $f_I$ on the top are shown in Figure 4(a) with dashed lines. There is a certain phase difference between the two series. As the maximum value and change speed of $f_I$ are larger than those of $f_D$, the wave force $f_H$ is dominated by $f_I$ and they almost reach the maxima simultaneously.

Figure 4(a) also shows the time series of $f_H$ at the heights of 5 m, 10 m, and 16 m, and it can be seen that the wave forces have similar phases and periods. The longer the distance from the calculated position to the seabed is, the larger the amplitude of $f_H$ becomes. Figure 4(c) further shows the change in the amplitude of $f_H$ along the height direction, and it can be seen that the growth rate gradually accelerates as the height increases and so does the water speed. For the single pile, the total maximum wave force $f_H$ is 154.18 kN.

When the pile length increases, the time series of $f_H$ on a single pile is computed in the same way, and the results are shown in Figure 5(a). For the five cases, the piles of the foundation are immersed in water, so they are completely subject to wave loads. With the increase in pile length from 16 m to 46 m, the period of the wave force on the pile remains the same but the amplitude increases gradually, i.e., 154 kN, 274 kN, 432 kN, 510 kN, and 669 kN, respectively, as shown in Figure 5(b). Moreover, it can be seen that the increasing range of the wave force is obviously larger than the increasing range of the pile length. For instance, the pile height increases by 1.88 times from the minimum to the maximum, but the wave force increases by 3.34 times. This phenomenon occurs because the water velocity increases with the increase in the distance from the calculated position

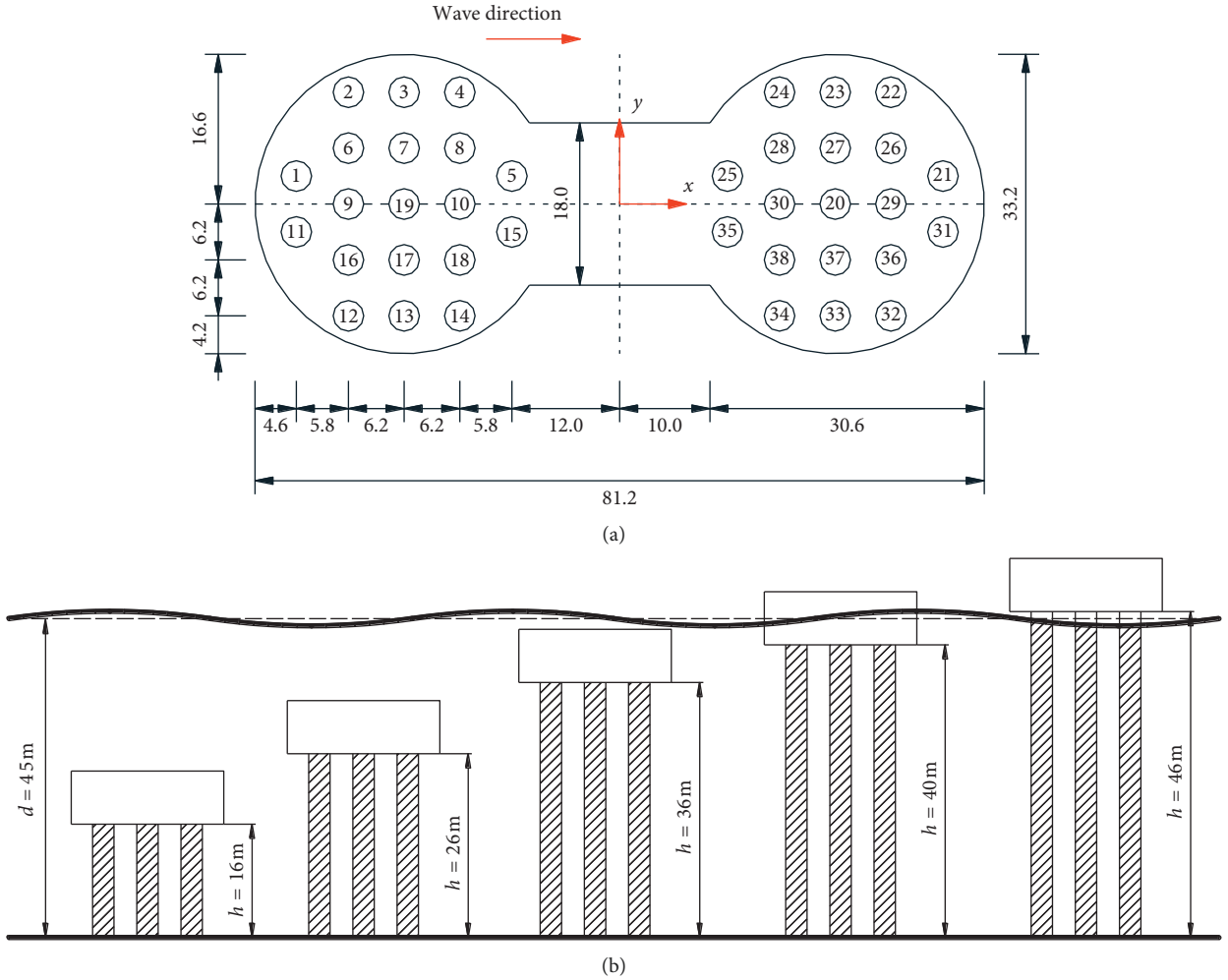


Figure 2: Computed pile foundations with different pile lengths. (a) Cross section. (b) Elevation.

to the seabed. As a result, the wave effect on the foundation with longer piles becomes more obvious, which is unfavourable to the structural stability.

The previous calculations of the wave loads focus on a single pile. However, there are 38 piles for N03 foundation, and the pile group effect has to be taken into account in the following analysis. To do this, the phase differences of the wave forces on the 38 piles are modified according to their spatial position relationships. Then, the group pile coefficient $K$, which is related to the ratio of the center distance $l$ between two adjacent piles to their diameter $D$, is introduced to consider the interference among piles. For the piles in parallel arrangement, that is, the vertical direction to the flow direction of water, the ratio $D/l$ is equal to about 2, so $K = 1.5$ is adopted according to the code [38]. For the piles in tandem arrangement, that is, the parallel direction to the flow direction of water, the shadowing effect of the upstream pile on the downstream pile is not considered conservatively, and $K = 1.0$ is adopted.

*2.3. Wave Forces on the Cap.* For the cap of the foundation, the dumbbell-type cross section is converted into a circular cross section based on area equivalent. The original cross-sectional area of the cap is 2,028.52 m$^2$, so the diameter $D$ of the equivalent circular cross section is equal to 50.8 m. As $D/L = 0.3 > 0.2$, the cap belongs to a large-scale structure on which the wave force could be calculated according to the method proposed by MacCamy and Fuchs. As shown in Figure 3(c), when the origin of the coordinate axis is set on the seabed, its forward wave force at a height of $z$ is expressed as follows:

$$F_H(z) = -\frac{2\rho g H}{k}\frac{\cosh kz}{\cosh kd}A(ka)\sin(\omega t - \alpha), \tag{4}$$

$$A(ka) = \frac{1}{\sqrt{\left[J_1'(ka)\right]^2 + \left[Y_1'(ka)\right]^2}}, \tag{5}$$

$$\tan\alpha = \frac{J_1'(ka)}{Y_1'(ka)}, \tag{6}$$

where $J_1'$ and $Y_1'$ are the derivatives of the first-order first-class and the first-order second-class Bessel functions, respectively; $a$ is the radius of the cap; and $\alpha$ is the phase lag angle.

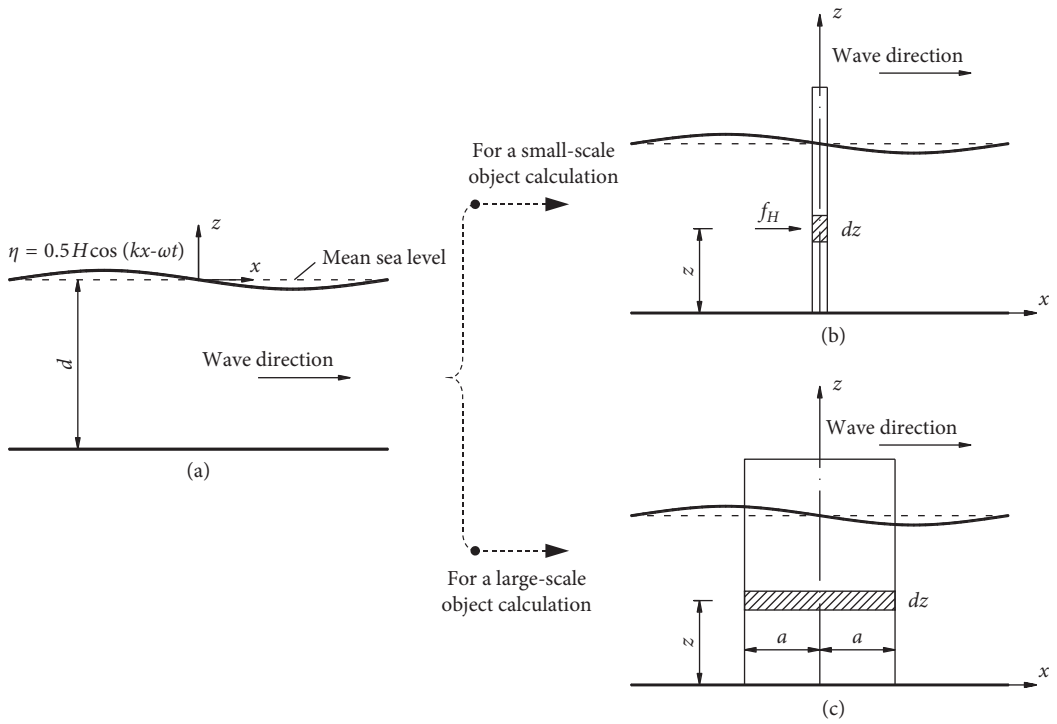


FIGURE 3: Computations of wave forces. (a) Schematic diagram of the linear wave theory. (b) For a small-scale object. (c) For a large-scale object.

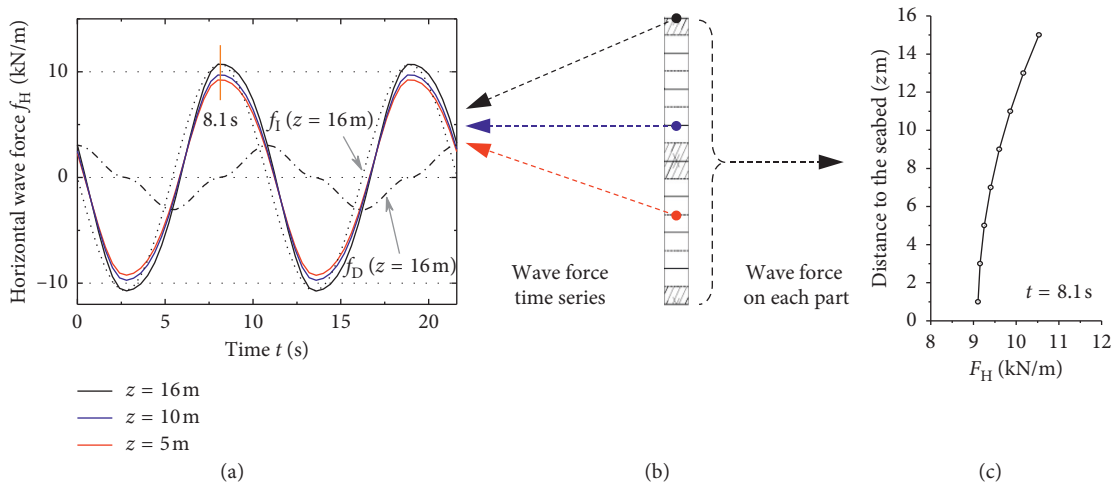


FIGURE 4: Horizontal wave forces on a pile. (a) Time series at different heights. (b) Schematic diagram of the division. (c) Maximum wave forces along the pile.

The time series of the wave force on the cap at different positions are shown in Figure 6(a). For the five cases, the maximum of $F_H$ is observed at 8.8 s as compared in Figure 6(b). When the cap is totally submerged in water, $F_H$ increases as the distance from the calculated position to the seabed increases and so does the water velocity. It can be seen that $F_H$ on the cap is larger than $f_H$ on a single pile obviously and is also larger than the total value of $f_H$ on all the piles. When the cap emerges from water, the wave force on the part exceeding sea level is no longer considered, and thereby $F_H$ decreases rapidly until the cap completely floats out of water and the wave force on the cap disappears. At this time, the wave force on the foundation is gradually dominated by $f_H$ on the piles.

## 3. Wave-Induced Response of the Foundation

*3.1. Structural Dynamic Characteristics.* Five finite element models of the foundation with different pile lengths are established using ANSYS software. Beam4 and Mass21 elements are adopted, and Figure 7 shows the first four modes including their modal shapes and frequencies. For each of

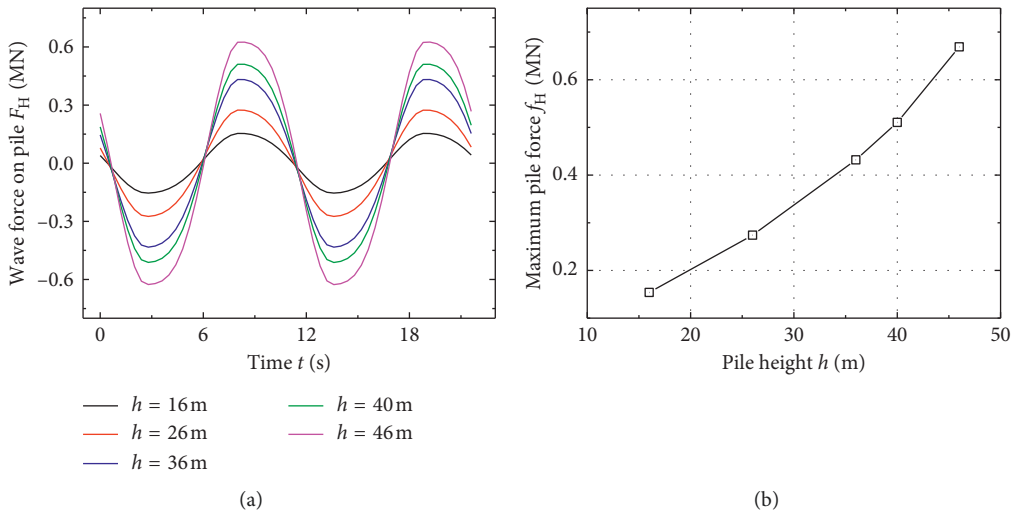


Figure 5: Total wave force on a pile with different lengths. (a) Time series. (b) Maximum values.

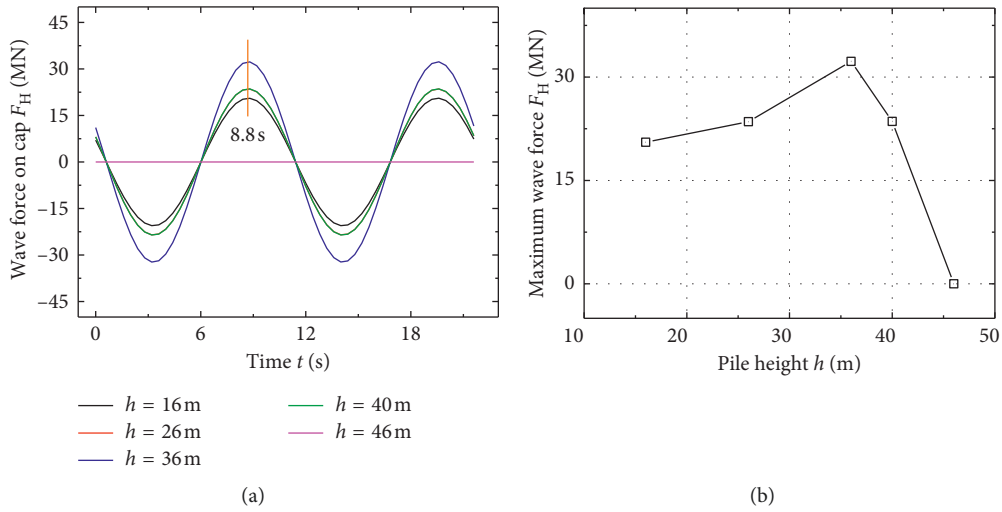


Figure 6: Total wave force on a cap with different pile lengths. (a) Time series. (b) Maximum values.

the five foundations, the first-order and the second-order modes correspond to the translations of the cap along $y$ axis and $x$ axis (Figure 2(a)), respectively. The frequencies of the two modes are close to each other, especially for larger pile lengths. When the pile length is larger than 36 m, the difference between the two frequencies is only about 0.1 Hz, so the wave-induced vibration could occur in both directions. The third-order and fourth-order modes correspond to the rotations of the cap around $x$ axis and $z$ axis, but they exchange with each other when the pile height is equal or larger than 26 m, indicating that the torsional stiffness around $z$ axis decreases more rapidly. As can be seen from Figure 7, with the increase in pile height from 16 m to 46 m, the fundamental frequency of the foundation significantly decreases from 2.82 Hz to 0.54 Hz. Although the fundamental frequency is still larger than the wave frequency, that is, 0.09 Hz, the foundation with longer piles obviously becomes flexible and is easier to be affected by the wave.

*3.2. Structural Response with Different Pile Lengths.* Under the action of the wave force, the response of the foundation with different pile lengths is analyzed using ANSYS software in the time domain. As is discussed in the introduction, the foundation can be regarded as a cantilever structure in the construction stage, so the response of the cap is the most obvious.

The results are shown in Figure 8, including the time series of the acceleration, the velocity, and the displacement at the top of the foundation. As can be seen from the figure, the time series include two components, the higher frequency response in the initial stage and the lower frequency response in the stable stage, which is particularly obvious in the acceleration series. The further spectrum analysis on the time series shows that the higher frequency is close to the fundamental frequency of the foundation, while the lower frequency is consistent with the wave frequency. This phenomenon can be verified by the damped structure model

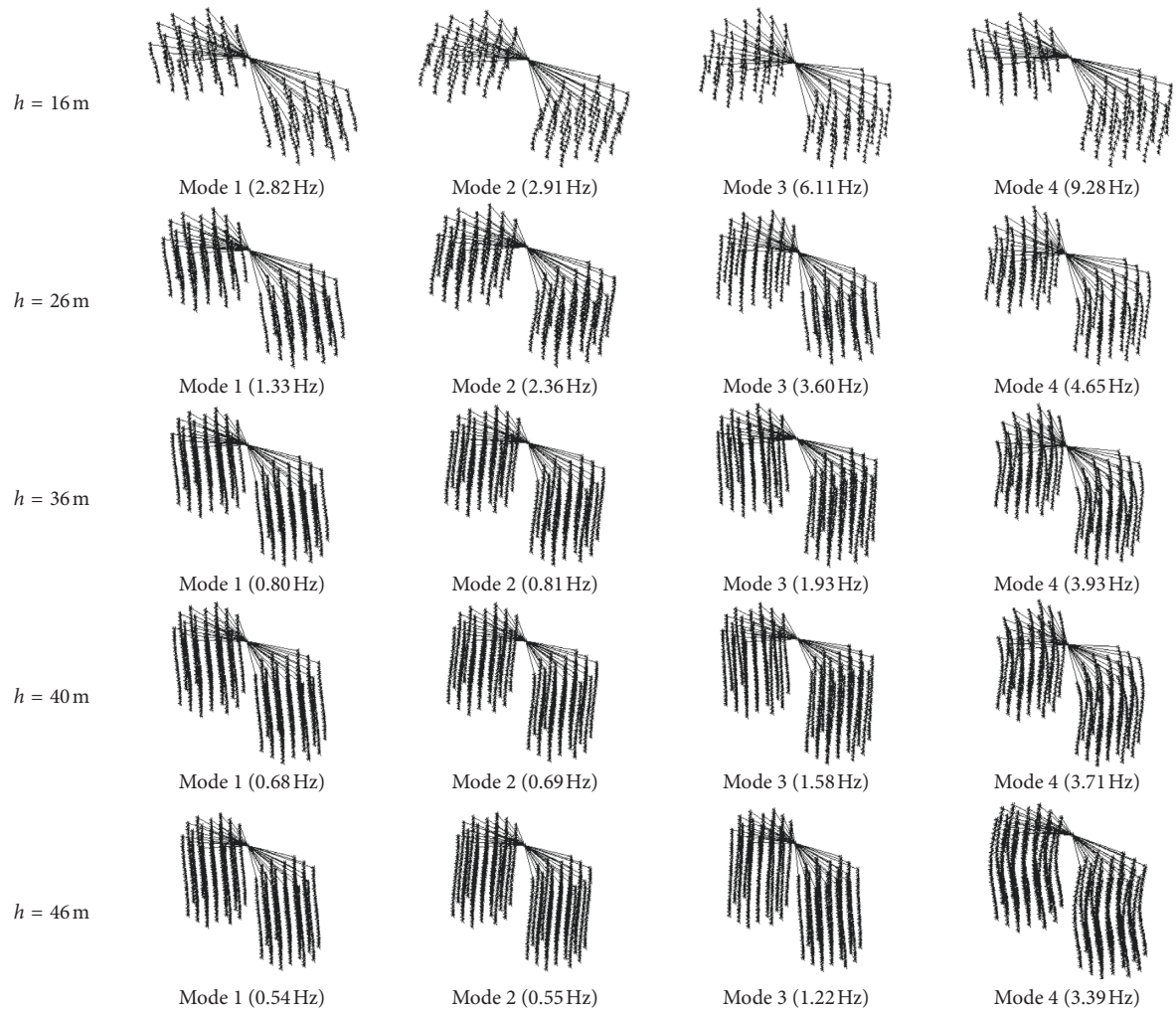


Figure 7: Dynamic characteristics of the foundations with different pile heights.

analysis in structural dynamics. Although the acceleration and velocity of the foundation vary greatly in the initial stage, the vibration is largely attenuated in the stable stage because there is no external energy input. The following study will focus the structural response in the stable stage.

The results show that the foundation with the pile length of 40 m when the cap partly emerges from water is the most sensitive to wave effects though the wave force on the cap decreases to some extent. One reason is that the wave forces on the piles continue to increase, and another reason is the foundation further becomes flexible. As a result, the maximum response of the foundation occurs in this situation. Moreover, the wave force on the cap is no longer considered when it emerges from water completely, and the time series of the acceleration and the velocity have multiple dominant frequencies.

Among the three parameters, the displacement response is the most intuitive parameter to evaluate the structural stability under the wave. It can be seen from Figure 8(c) that the amplitude of the displacement response of the cap increases from 1.46 mm when the pile length is 16 m to 39.5 mm when the pile length is 40 m but then decreases to 27.1 mm when the pile length is 46 m. For the piles, the maximum displacements are observed at their tops and are approximate to that of the cap due to the fixed connection. In the following study, therefore, the displacement response of the piles is omitted for brevity while the internal force response at the bottom is further studied.

The research begins with the comparison of the internal forces at the bottom for different piles. Taking the pile length of 16 m as an example, the peaks of the bending moments and the shearing forces of piles 1–5 (Figure 2(a)) on the upstream side and piles 31–35 on the downstream side are shown in Figure 9. For different piles, as there are phase differences in the wave forces, the corresponding times when the internal forces reach their peaks are different. The wave forces on the piles located in the middle have smaller phase differences from that of the cap, so these piles show higher internal forces. Among the ten piles, it can be seen that pile 35 has the maximum bending moment of 4.69 MN·m and the maximum shearing force of 0.64 MN. Pile 1 has the minimum bending moment of 4.43 MN·m and the

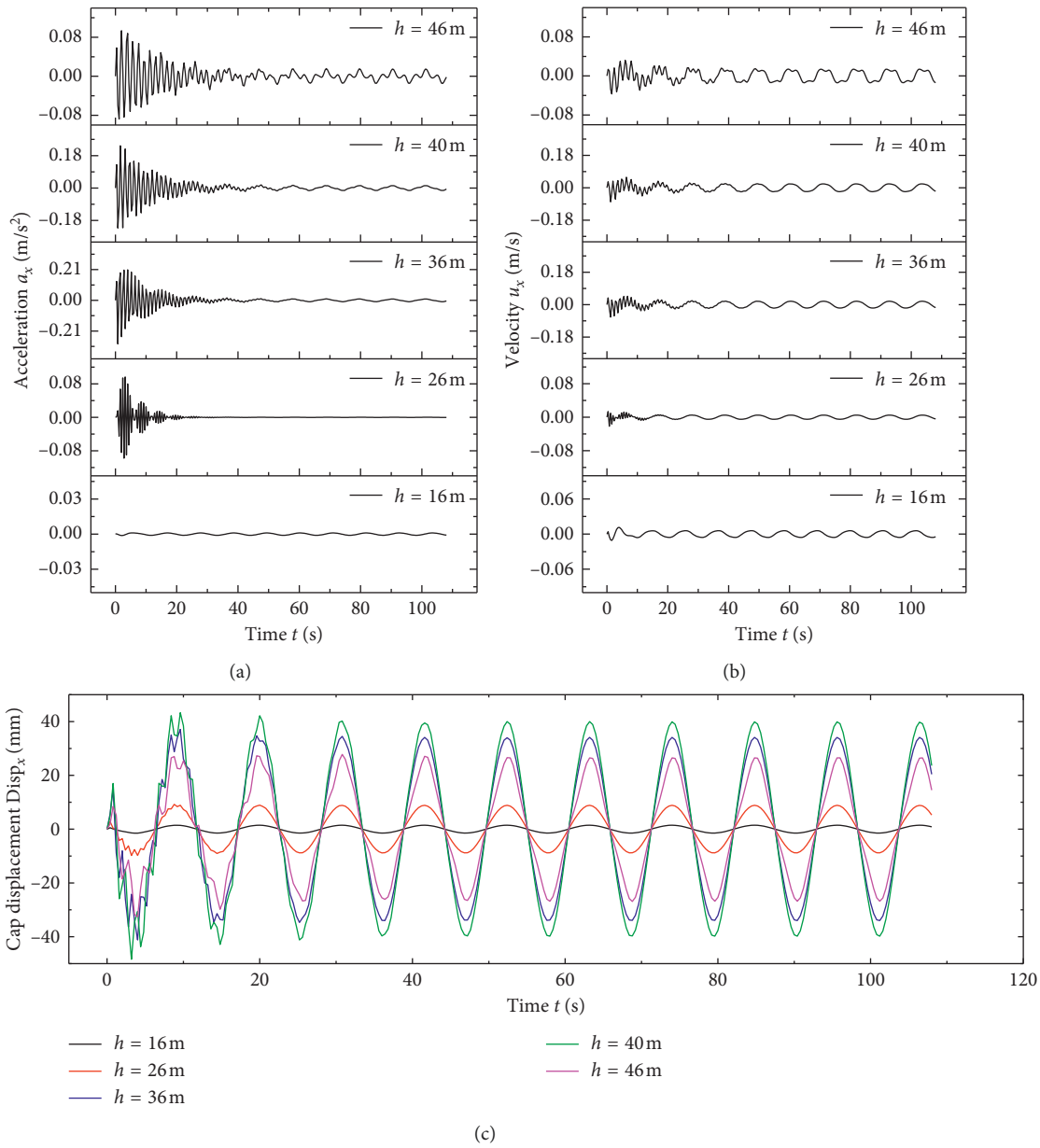


Figure 8: Response time series under the wave. (a) Acceleration. (b) Velocity. (c) Displacement.

minimum shearing force of 0.57 MN. Although Figure 9 shows only one peak of the time series, the results are typical because the internal force changes periodically.

Subsequently, the internal forces at the bottom for different pile lengths are compared. Taking pile 1 as an example, the time series of the bending moments and the shearing forces for the five foundations with different heights are shown in Figure 10. When the cap is totally submerged in water, the amplitude of the internal force increases with the increase in pile length. When the cap emerges from water partly, the amplitude of the internal force decreases, especially for the shearing force. When the cap completely floats out of water surface and the pile length is 46 m, the shearing force is even less than the value with the pile length of 16 m. It can be seen that the maximum internal force at the bottom is observed with the pile length of 36 m, while the maximum displacement at the top is observed with the pile length of 40 m. In other words, with the increase in pile length from 36 m to 40 m, the displacement response is further enhanced though the internal force has decreased, which verifies the adverse effect of the decreasing stiffness of the foundation, as discussed above.

In summary, the lower foundation with shorter piles shows better mechanical performance, and the wave-induced vibration is relatively small. However, the construction of this type of foundations is more complex. For instance, the lower foundation may require a bigger cofferdam. Such cofferdam also suffers from the wave and produces extra loads on the foundation, and an anchoring system may be necessary to keep the cofferdam stable. With

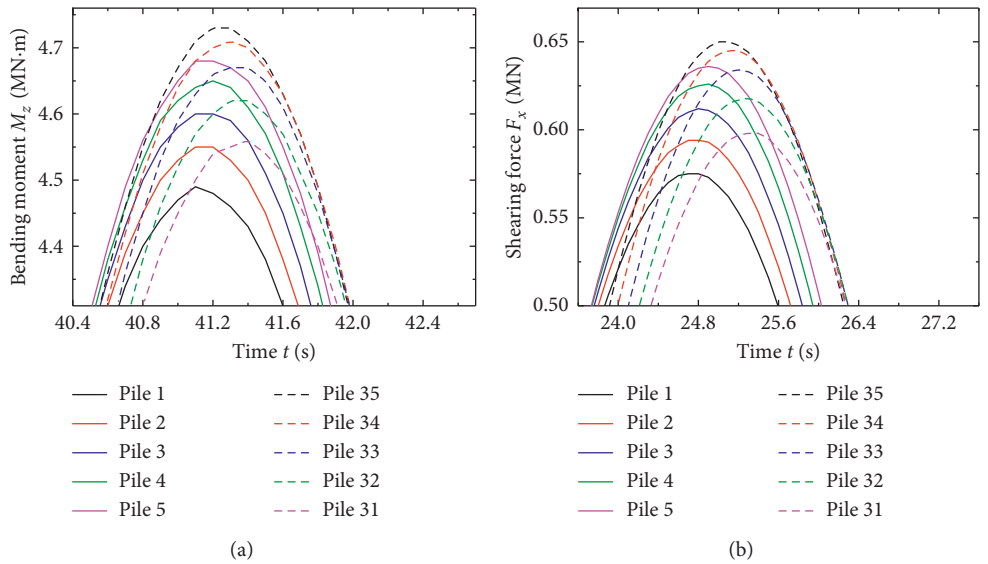


Figure 9: Internal forces of piles. (a) Bending moment. (b) Shearing force.

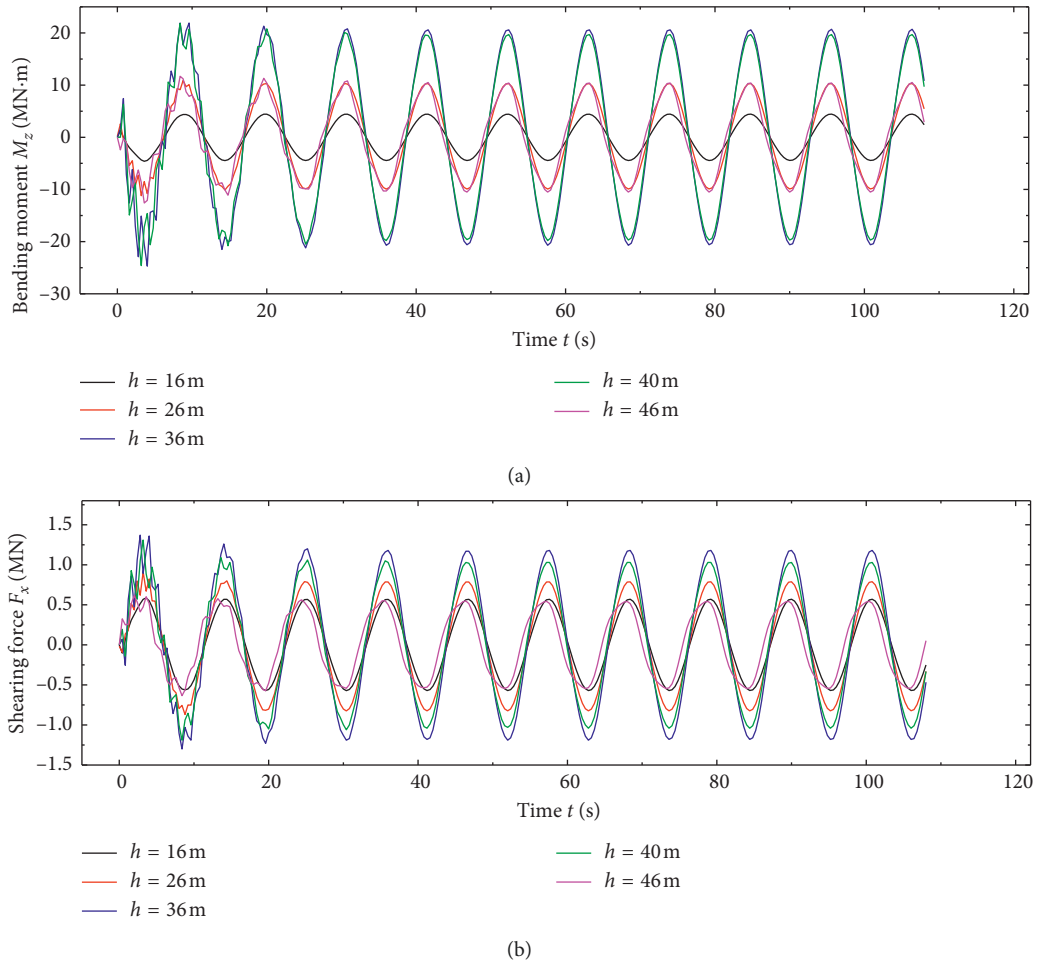


Figure 10: Internal forces of the five foundations. (a) Bending moment. (b) Shearing force.

the increase in pile length when the cap is close to or exceeds sea level, the difficulty in constructing the foundation may be reduced to some extent. However, the higher foundation with longer piles becomes more flexible and sensitive to the wave.

## 4. Optimization of the Foundation

*4.1. Structural Forms and Dynamic Characteristics.* To reduce deepwater operations and effects on navigation, the higher foundation with longer piles seems to be more suitable in deepwater areas with stronger waves. However, it can be seen from the previous analysis that the increase in pile length makes the structural stiffness decrease and so do the structural natural frequencies. Under the action of the wave, the dynamic response of the foundation is more obvious. Based on the understanding, reducing the free length of the pile may be favourable to improvement of the structural stability, and thereby three optimized forms are compared. Taking the foundation with the pile length of 36 m as an example, the first scheme is to set another cap at the center of the piles and is called the double caps foundation. The lower cap has a thickness of 8.0 m and the same cross-sectional size with the upper cap. The finite element model of the foundation adopts a double caps rigid frame structure. However, the wave force on the double caps foundation increases as the lower cap also suffers from the wave. In order to reduce the block area of the lower cap but not seriously weakening the overall rigidity of the foundation, the lower cap is divided into two separated caps with the diameter of 33.2 m. As there are three separated caps including one upper cap and two lower caps, this foundation is called the three caps foundation. In the third scheme, the separated lower cap is replaced by the steel lattice structure, which is installed among the piles and makes them into an integrated whole, to further reduce the block area, and this foundation is called the joint piles foundation. The steel lattice structure consists of many circular steel pipes with the diameter of 1 m and a thickness of 18 mm. The schemes of the three optimized foundations and the corresponding finite element models are shown in Figure 11.

The dynamic characteristics of the first four modes are listed in Table 1. The results show that the added structure could enhance the constraint on the foundation and improve its natural frequencies. The constraint effect of the double caps scheme is the most obvious, for the increases in the first four frequencies are the largest with an average percentage increase of 111.7%. The three caps scheme with the average percentage increase of 94.4% takes the second place. The joint piles scheme with the average percentage increase of 20.6% has the weakest constraint effect. For the first mode corresponding to the translation of the upper cap towards $y$ axis, the frequency is gradually increased with the increase in constraint effect. The improvement by the double caps scheme is the highest, but it is slightly higher than that of the three caps scheme. The trends of the second and the third modes, which correspond to the translation towards $x$ axis and the rotation around $z$ axis of the upper cap, are similar with that of the first mode. In particular, the lower cap in the double caps scheme connects the left pile group and the right pile group, so it has strong constraint on the rotation around $z$ axis and makes this modal to occur at a higher order. For the fourth mode corresponding to the rotation of the upper cap around $x$ axis, the frequency is still increased by the three optimized schemes. However, the effect of the double caps scheme becomes limited and is even less than that of the joint piles scheme. The probable reason is that the lower cap in the double caps scheme has the constraint effect, but the larger mass placed at the middle position with the maximum modal displacement makes the modal frequency to decrease at the same time.

*4.2. Wave Forces on Optimized Forms.* Since the three optimized foundations are obtained by installing the extra structures on the original foundation, the wave forces on the extra structures should be determined before analyzing their wave-induced response. For the joint piles scheme, the steel lattice members have a smaller diameter and shorter lengths when compared with the piles or the cap, so the wave forces on them are also smaller. The results show that the maximum wave forces on the members whose axes are vertical to the flow direction of water vary from 11 kN to 15 kN, while the members whose axes are parallel to the flow direction receive even less wave forces. Therefore, the wave force on the steel lattice structure is ignored. For the double caps and the three caps scheme, the wave forces on their lower caps are computed, as shown in Figure 12. Specifically, the upper and the lower caps in the double caps scheme have the same geometric dimension, so the wave forces on them have the same phase but different amplitudes. The maximum wave force on the lower cap is 18.50 MN, and the maximum wave force on the upper cap is 32.29 MN. The lower cap in the three caps scheme consists of two separated caps named as the upstream lower cap and the downstream lower cap according to the flow direction. As their values of $D/L$ are equal to 0.196 and less than 0.2, the separated caps belong to small-scale structures, and the Morison equation is suitable to calculate the wave forces on them. The maximum wave force on each of the two separated caps is 10.94 MN, but the total wave force has the maximum value of 13.8 MN due to the phase difference between the two caps. In summary, although the structural fundamental frequency increases, the optimized foundation is subject to a larger wave force, and it is necessary to understand which factor has more effects on the structural stability.

*4.3. Structural Response with Different Forms.* The wave-induced vibration of the optimized foundations is computed, and the time series of their displacements, bending moments, and shearing forces are shown in Figure 13. As can be seen from the figure, the higher frequency response is also observed in the initial stage, and it is close to the structural fundamental frequency. When the constraint effect of the extra structure increases and so does the structural fundamental frequency, the higher frequency response disappears gradually. Figure 13(a) compares the displacement response of the foundations with different

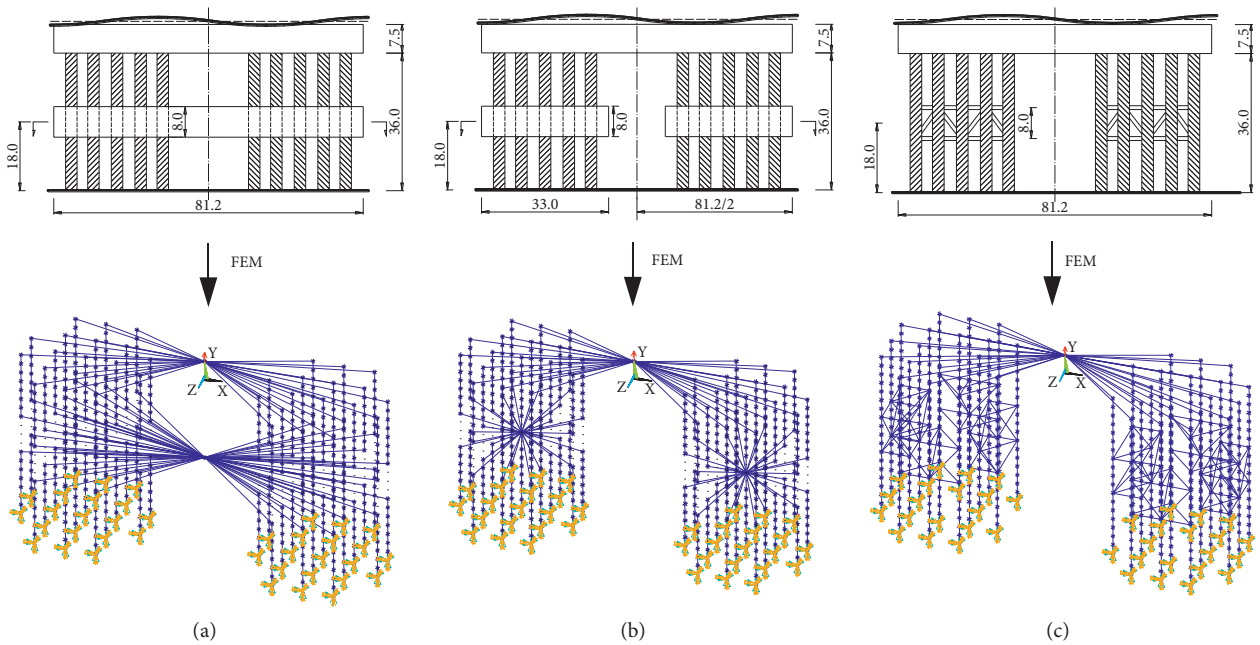


Figure 11: Optimized foundations (unit: m). (a) The double caps foundation. (b) The three caps foundation. (c) The joint piles foundation.

Table 1: Dynamic characteristics of the foundations with different forms

| Mode | Frequency (Hz) (modal shape) | | | |
|---|---|---|---|---|
| | Double caps foundation | Three caps foundation | Joint piles foundation | Original foundation |
| 1 | 1.87 (*T*-*y* axis) | 1.86 (*T*-*y* axis) | 0.99 (*T*-*y* axis) | 0.80 (*T*-*y* axis) |
| 2 | 2.11 (*T*-*x* axis) | 2.08 (*T*-*x* axis) | 1.04 (*T*-*x* axis) | 0.81 (*T*-*x* axis) |
| 3 | 4.08 (*R*-*x* axis) | 3.38 (*R*-*z* axis) | 2.41 (*R*-*z* axis) | 1.93 (*R*-*z* axis) |
| 4 | 5.55 (*R*-*y* axis) | 4.45 (*R*-*x* axis) | 4.14 (*R*-*x* axis) | 3.93 (*R*-*x* axis) |

*T* represents the translation of the upper cap towards *x* or *y* axis and *R* represents the rotation of the upper cap around *x*, *y*, or *z* axis.

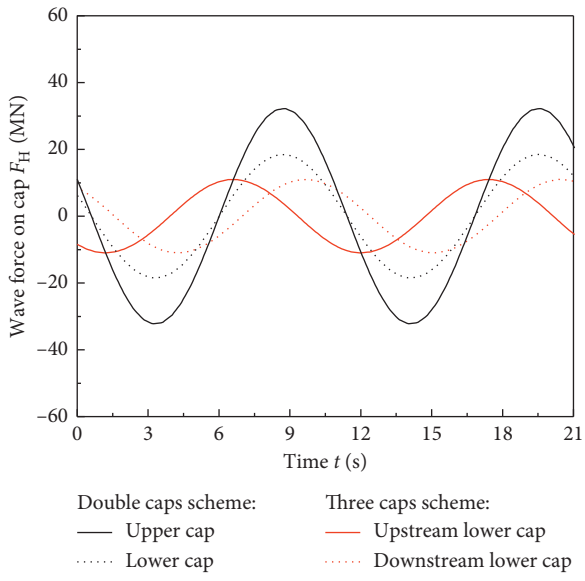


Figure 12: Wave forces on different caps.

forms at the tops. As the stiffness is improved after adding the lower cap or the steel lattice structure, the displacement response of the optimized foundations significantly decreases. The double caps foundation and the three caps foundation have almost the same performance for displacement optimization, and their percentage decreases of the maximum displacement are 86.2% and 85.9%, respectively. The joint piles foundation has weak effects on the displacement suppression, and its percentage decrease of the maximum displacement is 39.9%. Figure 13(b) compares the bending moment response of pile 1 at the bottom with different constraints. The optimized foundations effectively suppress their bending moments, especially for the three caps foundation with which the maximum bending moment decrease from the original value of 20.6 MN·m to 10.4 MN·m. Although the double caps foundation has better constraint effects, the larger wave force on the lower cap increases the maximum bending moment slightly. Figure 13(c) compares the shearing force response of pile 1 at the bottom with different constraints. However, the three optimized foundations all show adverse effects on their shearing forces. The maximum shearing force increases from 1.18 MN for the original scheme to 1.34 MN for the joint piles scheme, 1.49 MN for the three caps scheme, and 1.63 MN for the double caps scheme. Unlike the displacement and the bending moment response, the stronger the constraint effect on the foundation is, the larger the shearing force at the bottom becomes.

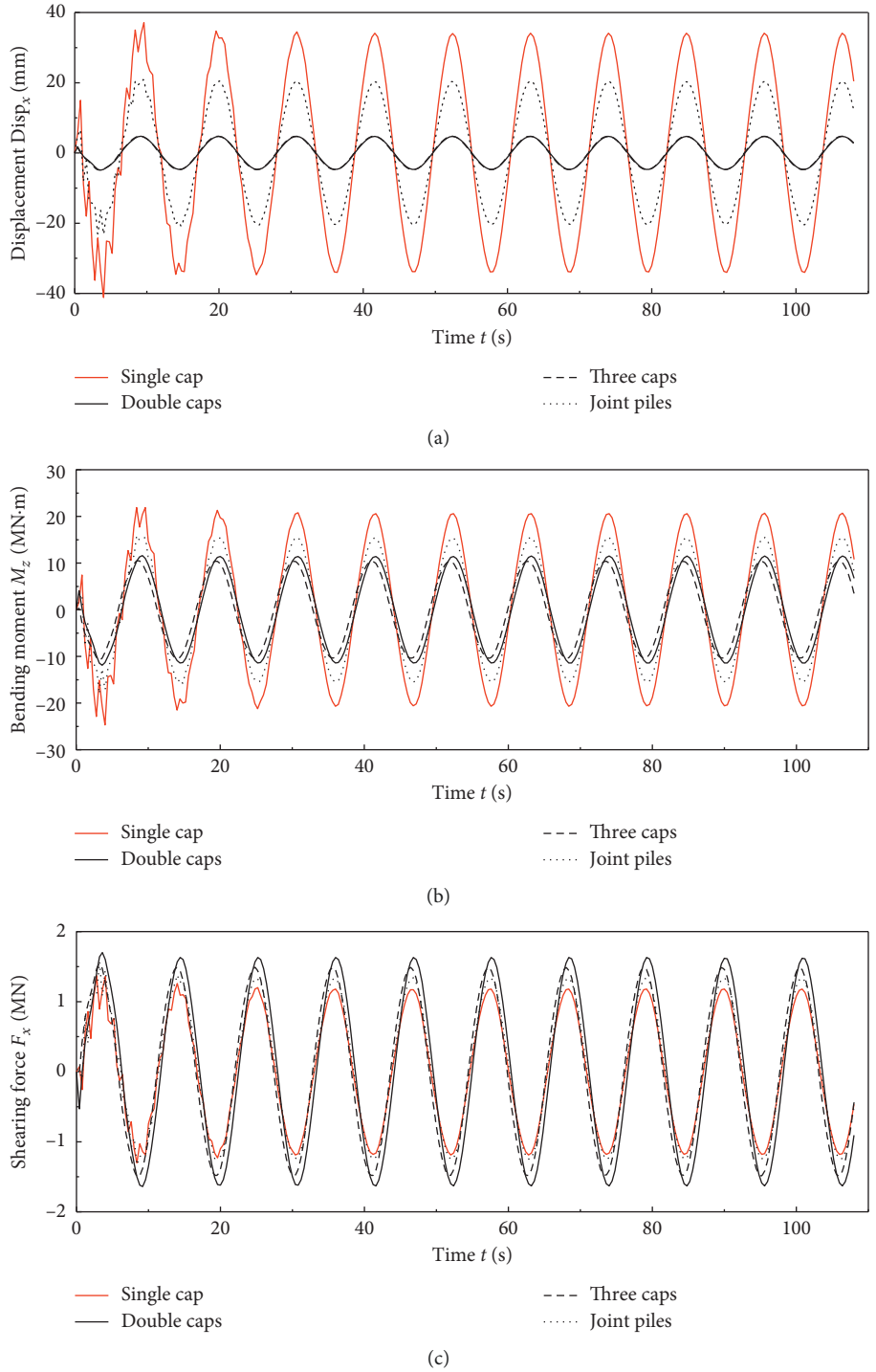


Figure 13: Response of different foundations. (a) Displacement. (b) Bending moment. (c) Shearing force.

Subsequently, the changes in bending moment and shearing force along pile 1 are studied, and the results for the three optimized foundations are shown in Figure 14. For the double caps scheme and the three caps scheme, due to the existence of the lower cap, the pile can be regarded as two parts, the upper one between the upper cap and the lower cap and the lower one between the lower cap and the ground. Each part can be regarded a member consolidated at its two sides where the internal forces are the maximum and the minimum, respectively. The bending moments at the two sides are opposite and change the sign in the middle position, while the shearing forces have the same sign. The bending moment of the lower part is larger than that of the upper part. The shearing force of the lower part is also larger due to the existence of the lower cap which increases the wave force on the foundation. For the joint piles scheme,

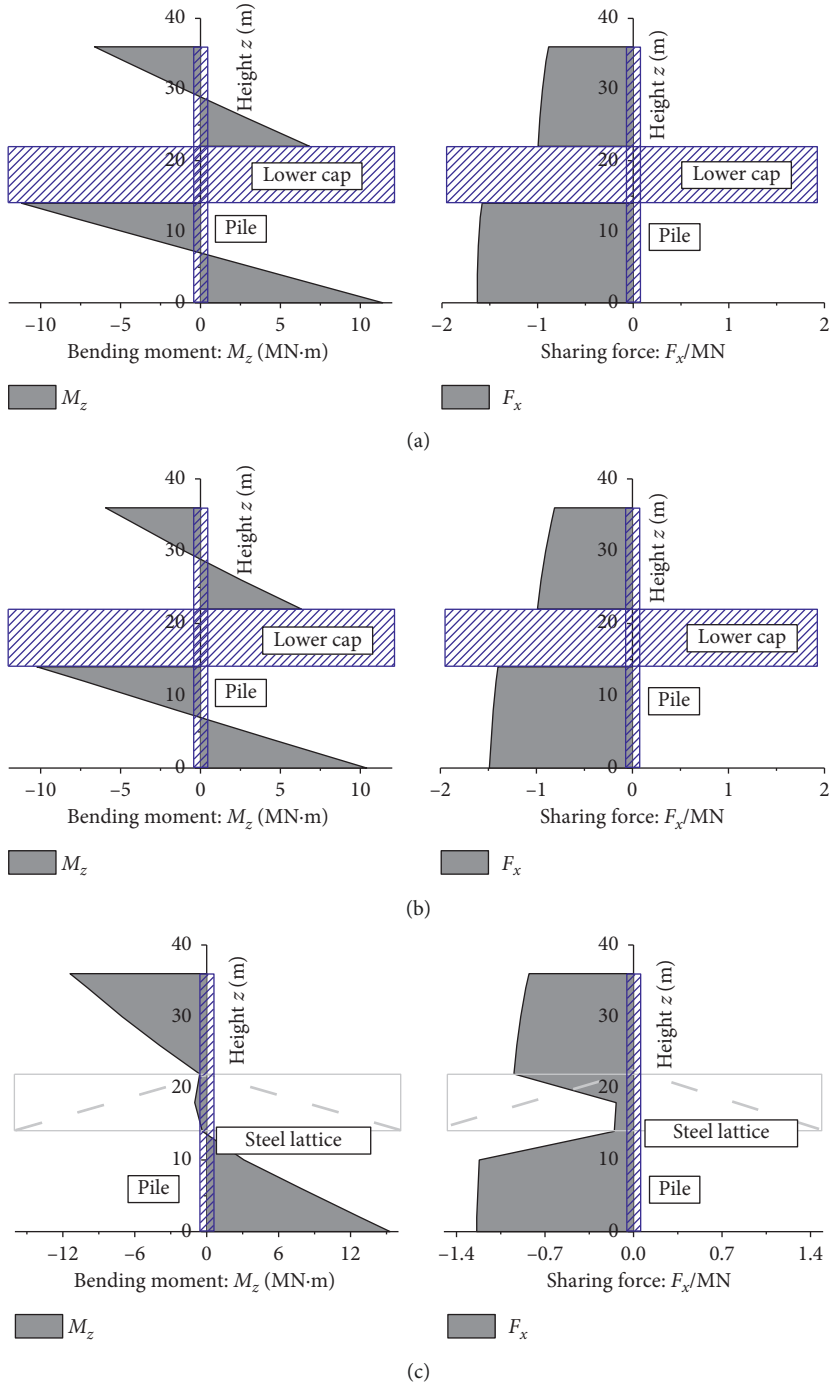


Figure 14: Comparison of internal forces on different foundations. (a) Double caps foundation. (b) Three caps foundation. (c) Joint piles foundation.

however, the distributions of the bending moment and the shearing force along the pile are different. It seems that the steel lattice structure provides an articulated constraint on the piles, as the bending moment in this region is close to zero.

## 5. Conclusions

This paper investigates the wave-induced response of a pile group foundation in deepwater area to improve the structural stability at the construction stage. The effects of the pile length and the structural form on the displacement and internal force of the foundation are studied, and the following main conclusions are made.

(1) For a determined water depth, the wave force on a pile increases with the increase in its length, and the increasing range of the former is obviously larger than that of the latter. Meanwhile, the wave force on

the cap also increases before it emerges from water and is larger than the total wave force on the 38 piles. On the contrary, the foundation with longer piles obviously becomes flexible, and its natural frequencies significantly decrease though the fundamental frequency is still larger than the wave frequency.

(2) The lower foundation with shorter piles shows better mechanical performance. The wave-induced response of the foundation including the displacement and the internal force is relatively small, but its construction may be more complex. The higher foundation with longer piles is convenient to the construction. As the wave force increases and the natural frequencies decrease, the foundation becomes more sensitive to the wave, especially when its cap partly emerges from water.

(3) All piles of the foundation have the same maximum displacement at the top where they are constrained by the rigid cap, but the time series of the internal forces have different amplitudes and phases. The internal force of a pile is larger when the wave force on the pile has a smaller phase difference from that of the cap. Setting a whole lower cap, two separated lower caps, or a steel lattice in the middle height of the foundation can reduce the free length of the pile and improve the structural frequencies to varying degrees. The lower cap and the steel lattice provide the consolidated constraint and the articulated constraint on the piles, respectively. Apparently, the lower cap has stronger constraint effects and decreases the displacement and the bending moment response of the foundation effectively. However, the wave force on the lower cap increases, which enhances the shearing force response.

(4) The study mainly focuses the wave-induced response of the foundation itself, while the practical construction conditions need to be considered as well when determining structural forms of pile group foundations of deepwater bridges.

## Data Availability

The data used to support the findings of this study are available from the corresponding author upon request.

## Conflicts of Interest

The authors declare that there are no conflicts of interest regarding the publication of this paper.

## Acknowledgments

The authors are grateful for the financial supports from the National Natural Science Foundation of China (51525804).

## References

[1] C. Fang, Y. Li, K. Wei, J. Zhang, and C. Liang, "Vehicle-bridge coupling dynamic response of sea-crossing railway bridge under correlated wind and wave conditions," *Advances in Structural Engineering*, vol. 22, no. 4, pp. 893–906, 2019.

[2] H. Tang, K. M. Shum, and Y. Li, "Investigation of flutter performance of a twin-box bridge girder at large angles of attack," *Journal of Wind Engineering and Industrial Aerodynamics*, vol. 186, pp. 192–203, 2019.

[3] G. B. Airy, *Tides and Waves*, Vol. 5, Encyclopedia Metropolitan, London, UK, 1845.

[4] G. Stokes, "On the theory of oscillatory waves," in *Transactions of the Cambridge Philosophical Society*, vol. 8, no. 310, pp. 441–473, 1880.

[5] T. Sarpkaya, M. Isaacson, and J. V. Wehausen, *Mechanics of Wave Forces on Offshore Structures*, Van Nostrand Reinhold Co., New York, NY, USA, 1981.

[6] M. M. Larmaei and T.-F. Mahdi, "Simulation of shallow water waves using VOF method," *Journal of Hydro-Environment Research*, vol. 3, no. 4, pp. 208–214, 2010.

[7] R. G. Dean and R. A. Dalrymple, *Water Wave Mechanics for Engineers and Scientists*, Prentice-Hall, Upper Saddle River, NJ, USA, 1984.

[8] G. H. Keulegan, "Spatially variable discharge over a sloping plane," *Transactions, American Geophysical Union*, vol. 25, no. 6, pp. 956–959, 1944.

[9] J. B. Keller, A. D. D. Craik, J. T. Stuart, P. L. Christiansen, and R. K. Bullough, "Soliton generation and nonlinear wave propagation," *Philosophical Transactions of the Royal Society A: Mathematical, Physical and Engineering Sciences*, vol. 315, no. 1533, pp. 367–377, 1985.

[10] Y. Xu, X. Xia, and J. Wang, "Calculation and approximation of the cnoidal function in cnoidal wave theory," *Computers & Fluids*, vol. 68, pp. 244–247, 2012.

[11] P. De Palma, M. D. de Tullio, G. Pascazio, and M. Napolitano, "An immersed-boundary method for compressible viscous flows," *Computers & Fluids*, vol. 35, no. 7, pp. 693–702, 2006.

[12] A. Sawicki and R. Staroszczyk, "Wave-induced stresses and pore pressures near a mudline," *Oceanologia*, vol. 50, no. 4, pp. 539–555, 2008.

[13] J. R. Morison, J. W. Johnson, and S. A. Schaaf, "The force exerted by surface waves on piles," *Journal of Petroleum Technology*, vol. 2, no. 5, pp. 149–154, 1950.

[14] R. C. MacCamy and R. A. Fuchs, "Wave forces on piles: a diffraction theory," Report No. 69, U.S. Army Corps of Engineers, Beach Erosion Board, Washington, DC, USA, 1954.

[15] F. Liu, S. Gao, H. Han, Z. Tian, and P. Liu, "Interference reduction of high-energy noise for modal parameter identification of offshore wind turbines based on iterative signal extraction," *Ocean Engineering*, vol. 183, pp. 372–383, 2019.

[16] B. Y. Dagli, Y. Tuskan, and Ü. Gökkuş, "Evaluation of offshore wind turbine tower dynamics with numerical analysis," *Advances in Civil Engineering*, vol. 2018, Article ID 3054851, 11 pages, 2018.

[17] S. Adhikari and S. Bhattacharya, "Dynamic analysis of wind turbine towers on flexible foundations," *Shock and Vibration*, vol. 19, no. 1, pp. 37–56, 2012.

[18] R. Zhang, Y. Tang, J. Hu, S. Ruan, and C. Chen, "Dynamic response in frequency and time domains of a floating foundation for offshore wind turbines," *Ocean Engineering*, vol. 60, pp. 115–123, 2013.

[19] K. Wei, S. R. Arwade, and A. T. Myers, "Incremental wind-wave analysis of the structural capacity of offshore wind turbine support structures under extreme loading," *Engineering Structures*, vol. 79, pp. 58–69, 2014.

[20] P. Wang, M. Zhao, X. Du, J. Liu, and C. Xu, "Wind, wave and earthquake responses of offshore wind turbine on monopile

foundation in clay," *Soil Dynamics and Earthquake Engineering*, vol. 113, pp. 47–57, 2018.
[21] E. Bachynski, M. Thys, and V. Delhaye, "Dynamic response of a monopile wind turbine in waves: experimental uncertainty analysis for validation of numerical tools," *Applied Ocean Research*, vol. 89, pp. 96–114, 2019.
[22] J. Sarmiento, A. Iturrioz, V. Ayllón, R. Guanche, and I. J. Losada, "Experimental modelling of a multi-use floating platform for wave and wind energy harvesting," *Ocean Engineering*, vol. 173, pp. 761–773, 2019.
[23] X. Wu, Y. Hu, Y. Li et al., "Foundations of offshore wind turbines: a review," *Renewable and Sustainable Energy Reviews*, vol. 104, pp. 379–393, 2019.
[24] K. Wei, W. Yuan, and N. Bouaanani, "Experimental and numerical assessment of the three-dimensional modal dynamic response of bridge pile foundations submerged in water," *Journal of Bridge Engineering*, vol. 18, no. 10, pp. 1032–1041, 2013.
[25] T. J. Ingham, S. Rodriguez, R. Donikian, and J. Chan, "Seismic analysis of bridges with pile foundations," *Computers & Structures*, vol. 72, no. 1-3, pp. 49–62, 1999.
[26] S. S. AbdelSalam, S. Sritharan, and M. T. Suleiman, "Current design and construction practices of bridge pile foundations with emphasis on implementation of LRFD," *Journal of Bridge Engineering*, vol. 15, no. 6, pp. 749–758, 2010.
[27] C. Liu, S. Zhang, and E. Hao, "Joint earthquake, wave and current action on the pile group cable-stayed bridge tower foundation: an experimental study," *Applied Ocean Research*, vol. 63, pp. 157–169, 2017.
[28] S.-x. Liu, Y.-c. Li, and G.-w. Li, "Wave current forces on the pile group of base foundation for the east sea bridge, China," *Journal of Hydrodynamics*, vol. 19, no. 6, pp. 661–670, 2007.
[29] W.-J. Yao, W.-X. Yin, J. Chen, and Y.-Z. Qiu, "Numerical simulation of a super-long pile group under both vertical and lateral loads," *Advances in Structural Engineering*, vol. 13, no. 6, pp. 1139–1151, 2010.
[30] Y. Deng, Q. Guo, and L. Xu, "Experimental and numerical study on modal dynamic response of water-surrounded slender bridge pier with pile foundation," *Shock and Vibration*, vol. 2017, Article ID 4769637, 20 pages, 2017.
[31] Y. Deng, Q. Guo, Y. I. Shah, and L. Xu, "Study on modal dynamic response and hydrodynamic added mass of water-surrounded hollow bridge pier with pile foundation," *Advances in Civil Engineering*, vol. 2019, Article ID 1562753, 23 pages, 2019.
[32] L. Deng, W. Yang, Q. Li, and A. Li, "CFD investigation of the cap effects on wave loads on piles for the pile-cap foundation," *Ocean Engineering*, vol. 183, pp. 249–261, 2019.
[33] L. Ya, C. Zekun, and N. Qinqin, "Dynamic response of pile-cap structure under random sea wave action," *Procedia Engineering*, vol. 116, pp. 1027–1035, 2015.
[34] K. Tomisawa and M. Kimura, "New technology on seismic reinforcement of pile foundation for long life bridges," *Procedia Engineering*, vol. 171, pp. 1035–1042, 2017.
[35] Z. H. Wang, R. Q. Xi, and G. X. Chen, "State of arts on response of bridge of pile foundation under earthquake excitation," *Journal of Nanjing University of Technology (Natural Science Edition)*, vol. 31, no. 1, pp. 106–112, 2009, in Chinese.
[36] A. G. Sextos, G. E. Mylonakis, and E.-K. V. Mylona, "Rotational excitation of bridges supported on pile groups in soft or liquefiable soil deposits," *Computers & Structures*, vol. 155, pp. 54–66, 2015.
[37] B. Le Méhauté, *An Introduction to Hydrodynamics and Water Waves*, Springer, New York, NY, USA, 1976.
[38] CCCC First Harbor Consultants Co Ltd., *JTS 145-2015 Code of Hydrology for Harbor and Waterway*, China Communications Press Co Ltd, Beijing, China, 2015, in Chinese.